Supplementary Materials for

Complement is activated by IgG hexamers assembled at the cell surface

Christoph A. Diebolder, Frank J. Beurskens, Rob N. de Jong, Roman I. Koning, Kristin Strumane, Margaret A. Lindorfer, Marleen Voorhorst, Deniz Ugurlar, Sara Rosati, Albert J.R. Heck, Jan G.J. van de Winkel, Ian. A. Wilson, Abraham J. Koster, Ronald P. Taylor, Erica Ollmann Saphire, Dennis R. Burton, Janine Schuurman, Piet Gros and Paul W.H.I. Parren.

Correspondence to: p.parren@genmab.com or p.gros@uu.nl

This PDF file includes:

Materials and Methods

Visualization of antibody structure and modeling of mutants.

Schematic views of the structure of human monoclonal antibody IgG1-b12 were generated from the 1HZH crystal structure using PyMOL version 1.5.0.4 (Schrödinger LLC). Mutant models were generated by selecting the rotamers closest to the original sidechain conformation using the mutagenesis module; no energy minimization was applied.

Construction, expression and purification of antibody variants.

Human monoclonal antibodies IgG1-7D8 recognizing CD20 (*18*), IgG1-005 recognizing CD38 (*19*), IgG1-2F8 recognizing EGFR (*33*) and IgG1-b12 recognizing HIV-1 gp120 (*34*) were used as model antibodies with G1m(f) allotypes. Codon-optimized antibody genes (GeneArt, Germany) were cloned in pConG1f (Lonza) for 7D8 heavy chain variants, pConKappa (Lonza) for the 7D8 light chain, and pcDNA3.3 (Invitrogen) for heavy and light chain variants of 005, 2F8 and b12. Isotype variants were generated as described previously (*35*). Isotypic variants were based on human IgG2 (Uniprot entry P01859), IgG3 (P01860) and IgG4 (P01861). Mutations were introduced in heavy chain expression vectors using Quikchange technology (Agilent Technologies, US) at positions numbered according to Eu nomenclature. Antibodies were expressed in HEK293 FreeStyle cells by transfection of light chain and heavy chain expression vector DNA using 293fectin essentially as described by the manufacturer (Invitrogen, US). Antibodies were purified by Protein A affinity chromatography (rProtein A FF; GE Healthcare), dialyzed overnight against PBS, and filter-sterilized over 0.2-µM dead-end filters. Concentration of purified IgGs was determined by absorbance at 280 nm. Quality assessment of purified antibodies was performed by SDS/PAGE, mass spectrometry, and HP-SEC. Bispecific molecules were generated by controlled Fab arm exchange of the purified homodimeric components in the presence of 25 mM 2-MEA as described (*21*). The functionally monovalent bispecific antibodies directed against CD20 and the, for this experiment, innocuous antigen HIV-1 gp120 (IgG1-7D8/b12) or against EGFR and HIV-1 gp120 (IgG1-2F8/b12), were generated by controlled Fab arm exchange of IgG1-b12-F405L with IgG1-7D8-K409R and with IgG1-2F8-K409R, respectively.

Cell culture and reagents.

A431 cells (human epidermoid cell line) were obtained from the Deutsche Sammlung von Mikroorganismen und Zellkulturen (cell line number ACC 91; Braunschweig, Germany). Daudi, Raji and Ramos cells (human Burkitt's lymphoma) were obtained from the American Type Culture Collection (ATCC no. CCL-213, CLL-86 and CRL-1596 respectively; Rockville, MD). HEK293 Freestyle cells were obtained from Invitrogen (Paisley, UK). All cell lines were routinely tested for mycoplasma contamination and generally aliquoted and banked to allow *in vitro* assays to be performed from frozen cell stocks and not from continuous cultures to ensure authenticity of the cells. Pooled normal human serum (NHS) AB was obtained from Sanquin (The Netherlands), C1q-depleted serum from Quidel (San Diego, CA) and C4-depleted serum from Complement Technology Inc (Tyler TX). Purified C1 was provided by M. Daha (Leiden University Medical Center, Leiden, the Netherlands) and C1q was purchased from Complement Technology Inc. The Fc binding peptide DCAWHLGELVWCT (*17*) and control peptide GWTVFQKRLDGSV were synthesized by Pepscan Presto B.V. (Lelystad, The Netherlands).

Determination of C1q binding to antibody-opsonized cells.

Determinations of C1q binding to B cells pre-reacted with CD20 antibodies was performed as described (*27*).

CDC assays.

CDC assays were performed as described (*27*), either with a fixed antibody concentration of 10 µg/mL in C1q-deficient serum supplemented with a concentration series of C1q, or with an antibody concentration series or a fixed antibody concentration and normal human serum (20% final concentration) as a source of complement. Killing was calculated as the % PI+ cells determined by a BD FACSCanto II flow cytometer for Daudi, Raji and Ramos B cells, and as % TOPRO-iodide+ cells determined by a Celigo imaging cytometer (Brooks Life Science Systems) for A431 carcinoma cells.

CDC assay with Fc-binding peptide or irrelevant peptide.

Raji or Daudi cells were incubated with a fixed concentration of IgG1-7D8 (6 µg/mL) or IgG1-005 (0.8 µg/mL), respectively and the Fc binding peptide DCAWHLGELVWCT or control peptide GWTVFQKRLDGSV at a final concentration of 60 µg/mL with normal human serum (20% final concentration) as a source of complement. Killing was calculated as the % PI+ cells determined by a BD FACSCanto II flow cytometer.

Solution-phase complement activation assay.

Complement activation in the absence of target was determined by measuring C4d concentrations, a marker for classical pathway complement activation, after incubating 100 µg antibody in 1 mL 90% normal human serum for 1 hour at 37ºC. C4d concentrations were measured in an ELISA (MicroVue C4d EIA kit, Quidel Corporation, San Diego, US) according to the manufacturer's instructions.

HP-SEC analysis.

HP-SEC fractionation was performed using a Waters Alliance 2975 separation unit (Waters, Etten-Leur, The Netherlands) connected to a TSK HP-SEC column (G3000SW_{xl}; Toso Biosciences, via Omnilabo, Breda, The Netherlands), a Waters 2487 dual λ absorbance detector (Waters), and a Mini Dawn Treos MALS detection unit (Wyatt). 50 µL samples containing 1.25 µg/mL protein were separated at 1 mL/min in 0.1 M Na_2SO_4 /0.1 M sodium phosphate buffered at pH 6.8. Results were processed using Empower software version 2002 and expressed per peak as percentage of total peak area.

Native mass spectrometry.

IgG1 oligomerization was studied by native mass spectrometry as described previously (*36*). The constructs were analyzed in 0.05 M ammonium acetate (pH 7.0) at an antibody concentration of 5 µM. This protein preparation was obtained by five sequential concentration and dilution steps at 4ºC using a centrifugal filter with a cut-off of 10 kDa (Millipore). Samples were sprayed from borosilicate glass capillaries and analyzed on a modified quadrupole time-of-flight instruments (Waters, UK) adjusted for optimal performance in high mass detection (*37, 38*). Instrument settings were as follows; needle voltage ~1.4 kV, cone voltage ~150 V, source pressure 9 mbar. Extent of oligomerization was estimated by summing the areas under the curves. We analyzed wild type IgG1-005 and triple mutant IgG1-005-RGY in parallel. Peak

intensities may have been affected by ionization and transmission efficiency of the different protein species and therefore did not directly represent relative abundance.

Negative stain electron microscopy.

4 µL of IgG1-005-RGY (30 µg/mL) was applied to a glow discharged EM grid with continuous carbon film and stained with 3% uranyl-acetate solution as described previously (*39*). Electron tomograms were acquired using a Tecnai F20 (FEI) electron microscope, equipped with FEI 4k x 4k Eagle CCD camera at 200 kV. 50,000 x magnification resulting in a pixel size of 4.4 Å at specimen level and a nominal defocus of -1 µm were applied. Tomograms were reconstructed and visualized in IMOD (*40, 41*) after low-pass filtering to the first zero of the CTF (~2 nm). 237 subtomograms of hexamers were boxed for averaging in PEET (*42*). The final average comprising 200 particles had a resolution of 2.9 nm according to the 0.5 FSC criterion.

Sample preparation for cryo-electron tomography.

Incubations of DNP-labeled liposomes and anti-DNP antibody (Wako Diagnostics, Richmond, VA) with purified C1, C4-depleted human serum and normal human serum were performed as described previously for liposome immune assays for measuring total complement activity of reconstituted complexes (*43*). Purified bovine C1 was provided by Dr. M. Daha. Samples for cryo-ET were prepared by plunge freezing. EM grids, R1.2 1.3, Cu, 200 mesh (Quantifoil), were glow discharged for 1 min at 30 mA and negative polarity using a K950X carbon coater (Emitech). Protein conjugated 6 nm gold particles (Aurion) were added as fiducial markers. Grids were blotted 3 s with filter paper (Whatman 541) and vitrified in a propane/ethane (2:1 v/v) mixture using a EM GP (Leica) at 95% humidity at room temperature.

Single and dual axis cryo-electron tomography.

Single axis cryo-electron tomography tilt series were acquired using Gatan 626 or Gatan 914 high-tilt cryo-holders on a Tecnai F20 (FEI), equipped with FEI 4k x 4k Eagle CCD camera and a GIF (Gatan) operated at 200 kV. Low-dose tilt series comprising 51 images were acquired in a range of +/- 60° in continuous Saxton tilt scheme at an initial increment of 3°, using tilt-angle dependent exposure times. Initial microscope magnification of 29,000 x using a 2x binned 4k x 4k FEI Eagle CCD camera resulted in a pixel size of 7.6 Å at specimen level. The total dose was 10,000 e^-/nm^2 or ~5,100 e^-/nm^2 per tilt series. Auto focusing was performed every second tilt angle at ~ 5 micron distance. Tilt series were taken at -5 to -7.5 micron defocus resulting in a first zero of the contrast transfer function (CTF) between 3.5 nm and 4.3 nm. Dual-axis tilt series were acquired in a similar manner using a FEI Titan Krios at 200 kV acceleration voltage and parallel illumination with a GATAN Quantum imaging filter. The total electron dose was 10,000 e^-/nm^2 per dual-tilt series.

Image processing.

Cryo-electron tomograms were reconstructed using IMOD version 4.5.3 (*40, 41*). The defocus was measured using TOMOCTF (version Dec 2009 (*44*)) and CTF correction was applied by phase flipping in IMOD. 3D volumes were reconstructed applying five iterations of SIRT (*45*), while applying a low pass filter to ~1.3 nm resolution. Dual axis data sets were combined using manually prealigned reference points in separately reconstructed single tilt tomograms (*41*). PEET (*42*) was used for subtomogram averaging. Binary particle masks were created in SPIDER (*46*). 230 particles were pre-aligned using the PEET program stalkInit. The

average of pre-oriented particles was used as an initial reference for alignments. Principle component analysis and k-means clustering for classification were performed on 200 best particles (*47*). The three main structure factors were used for separation into seven clusters (fig. S4B). The main class of 111 particles contained 107 particles obtained from tomograms of C4-depleted serum, which were used for final analysis (fig. S4D). After symmetrization in IMOD and volume estimation using VADAR (*48*), atomic structures for IgG1-b12 antibody (1HZH (*15*)), globular head domains of C1q (1PK6 (*49*)), collagen (1CGD (*50*)) and C1rs (1NZI (*51*); 3DEM (*52*); 3POB (*53*)) were docked into the EM map by hand and refined using SITUS collage (*54, 55*). IMOD and UCSF Chimera (*56*) were used for visualization.

Adaptation of the 1HZH hexamer structure for docking.

To dock the 1HZH crystal packing arrangement in the lower platform of the cryo-ET density map, we adapted the alternating up-down pattern of Fab arms in neighboring antibodies (fig. S5A). Orienting all six axial Fab segments downwards left the central hexameric Fc ring unchanged (fig. S5, B and D) and fitted the IgG model in the observed lower platform by creating a table-like arrangement with Fc segments and six Fab arms equatorial and six Fab arms pointing downwards (Fig. 4F, fig. S5C).

Modeling of the antibody-C1 complex.

The ~6 nm resolution was too low for direct automated docking of high-resolution crystal structures. Initial manual placement of components (hexameric Fc ring, 12 Fabs, six C1q headpieces and collagen stalks, and a premodelled $C1r_2s_2$ platform) was guided by structural details and orthogonal biochemical data that were available. Comparison of a number of simulations (fig. S4, H and I) indicated that the lower platform was best modeled by the hexameric IgG ring with incomplete binding of four C1q headpieces, accounting for the four discernible densities on top of this platform (Fig. 4C, fig. S4I). Positioning the C1q headpieces on the rim of the Fc ring was consistent with independent computational modeling of Fc-C1q headpieces based on available mutagenesis data (*57*).

To prepare a model of the complete C1-antibody complex, we applied six-fold symmetry to fill in the two missing C1q headpieces (fig. S4, fig. S6). Keeping the hexameric Fc ring fixed, we manually fitted six globular C1q headpieces, each associated sideways with an equatorial Fab into the main globular densities of the lower platform. In this model, C1q contacted the Fc segment in a manner that was consistent with binding of the globular head to the C_H2 domain of IgG as previously proposed (*57*). For each IgG, one Fab arm was bound to the surface antigen DNP, whereas the other Fab and Fc interacted with C1q (fig. S6C). From the non-symmetrized average density of the C1-antibody complex, four of these interactions could be readily discerned, whereas disorder was apparent at the remaining two positions (Fig. 4C; fig. S4I). The manual placement of the individual atomic models was improved from 7.4% correlation to a converged value of 13.3% after 10 rounds of Powell optimization using Situs collage (*54, 55*).

The six globular and trimeric C1q headpieces are connected to each other through collagenous triple-helices that form a bundle at the N-terminus (*49, 58*). While the 14-nm long collagenous stems were not resolved in the averaged map, density was observed for the 10nm bundle on top of the upper platform (Fig. 4, A and B). We modeled the stems as direct connections between the density of the bundle to the center of the globular densities of the lower platform; this resulted in an angle of 40º between the bundle and the stems (fig. S6E), which was in agreement with neutron scattering of C1q (*59*). To model the proteases C1r and C1s, we

applied two-fold symmetry to the upper platform corresponding to their presumed hetero-tetrameric arrangement. The N-terminal domains were inserted in a planar arrangement, with the proposed collagen-binding sites on C1r and C1s in close proximity to the six collagen stems (fig. S6, D and E), consistent with Bally et al. (*60*) and Phillips et al. (*61*). We did not observe any density for the C-terminal domains of C1r and C1s. Presumably, flexibility of the linker domains connecting the serine protease domains to the N-terminal base (*62*) resulted in absence of density.

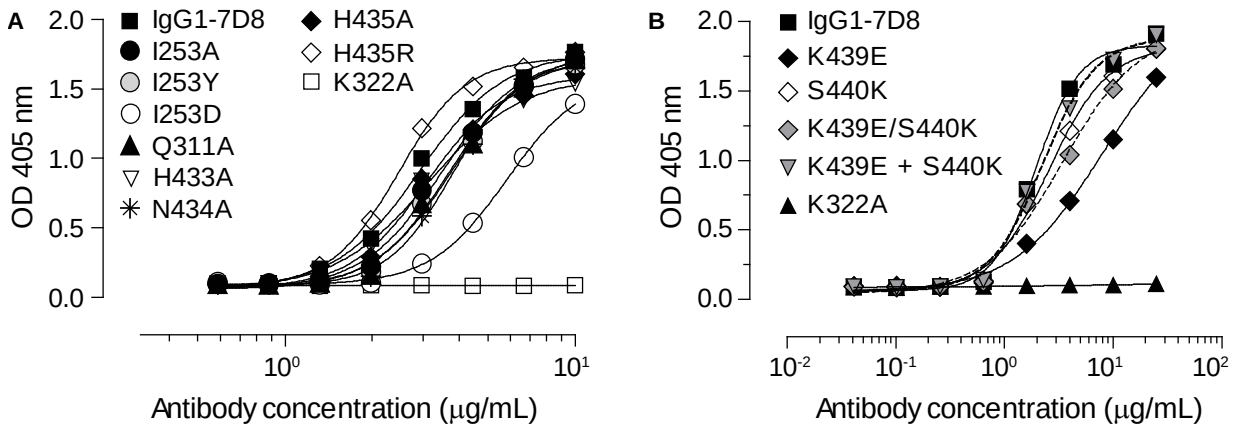

Fig. S1

C1 binding to immobilized IgG1-7D8 assessed by enzyme-linked immunosorbent assay (ELISA). Wild type IgG1-7D8 and IgG1-7D8 variants carrying amino acid mutations were randomly immobilized on microtiter plates. Binding of C1 captured from 3% pooled human serum and detected with rabbit anti-human C1q is shown. A K322A mutant abrogating C1 binding was used as a negative control. C1 binding was minimally (I253D and K439E) or not affected (all other mutants) as compared to wild type IgG1-7D8. (**A**) and (**B**) show a comparison of wild type IgG1-7D8 with a different set of mutants. Representative examples are shown (*N*=3).

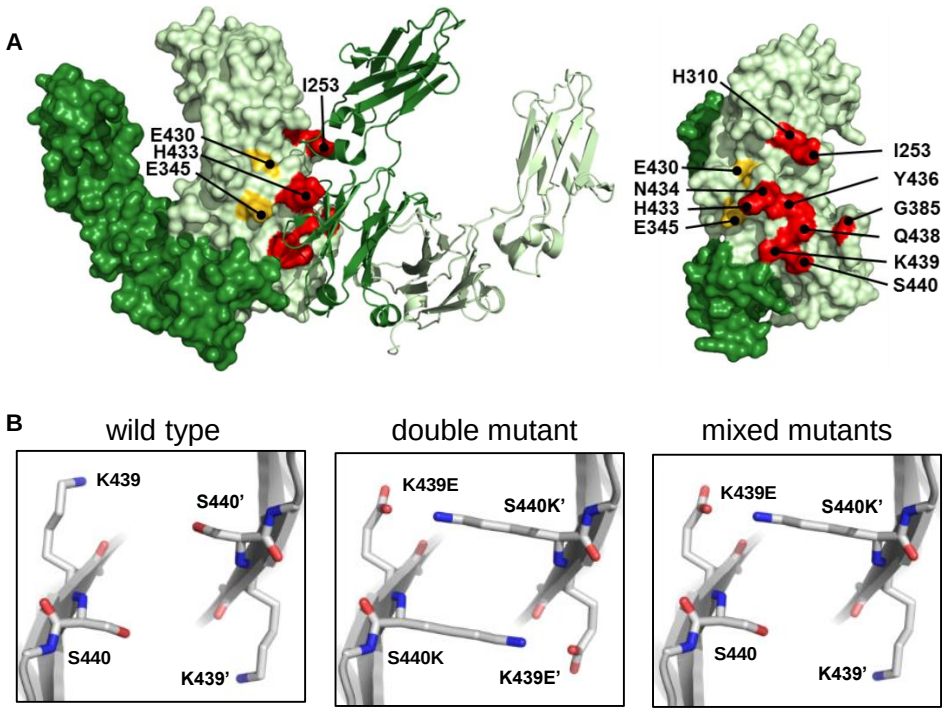

Fig. S2

Models indicating residues critical for Fc:Fc interactions. (**A**) Surface map of an IgG1 Fc segment and a ribbon cartoon representing a neighboring antibody Fc segment. Red and yellow indicate residues with mutations that decreased or enhanced complement activation respectively (Fig. 1, E,F and G; table S2). (**B**) Left: detail from the hexamer structure 1HZH, which indicated that residue K439 faces residue S440 on the complementary Fc segment of a neighboring antibody. The middle and right panel show modeled interactions for a K439E/S440K double mutant and a mixture of K439E and S440K single mutants. The modeling suggested that the alignment of positive and negative charges between neighboring Fc segments would negate repulsion for the double mutant (middle) or the single mutant mixture (right).

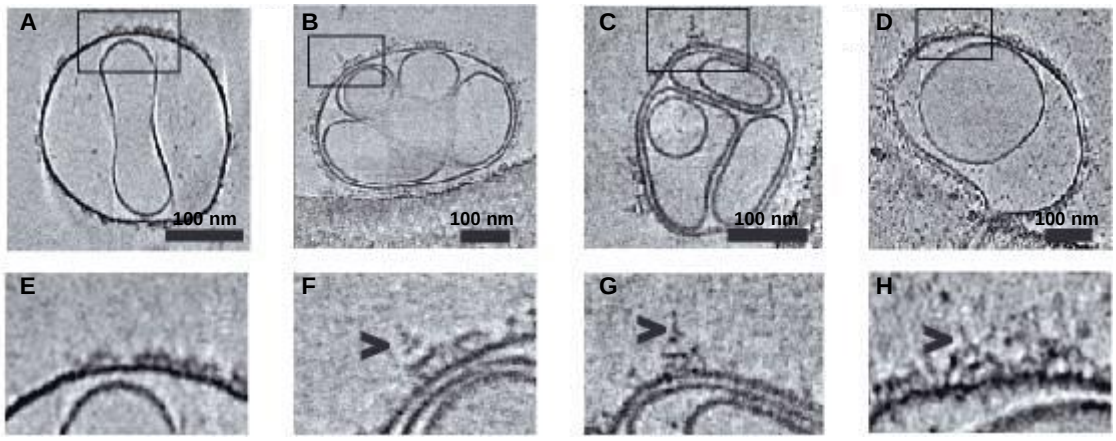

Fig. S3

Cryo-ET imaging of complement activation steps on DNP-labeled liposomes. Sections shown represent DNP-labeled liposomes incubated with: (**A**) anti-DNP antibody alone, (**B**) anti-DNP antibody and purified C1, (**C**) anti-DNP antibody and C4-depleted serum (complement activation arrests at C1), (**D**) anti-DNP antibody and normal human serum (resulting in a ~25-nm thick crowded layer covering the liposomes). (**E** to **H**) Represent enlargements of the areas indicated by a rectangle in the image above. Arrowheads point to antibody-C1 complexes with a height of ~ 33 nm.

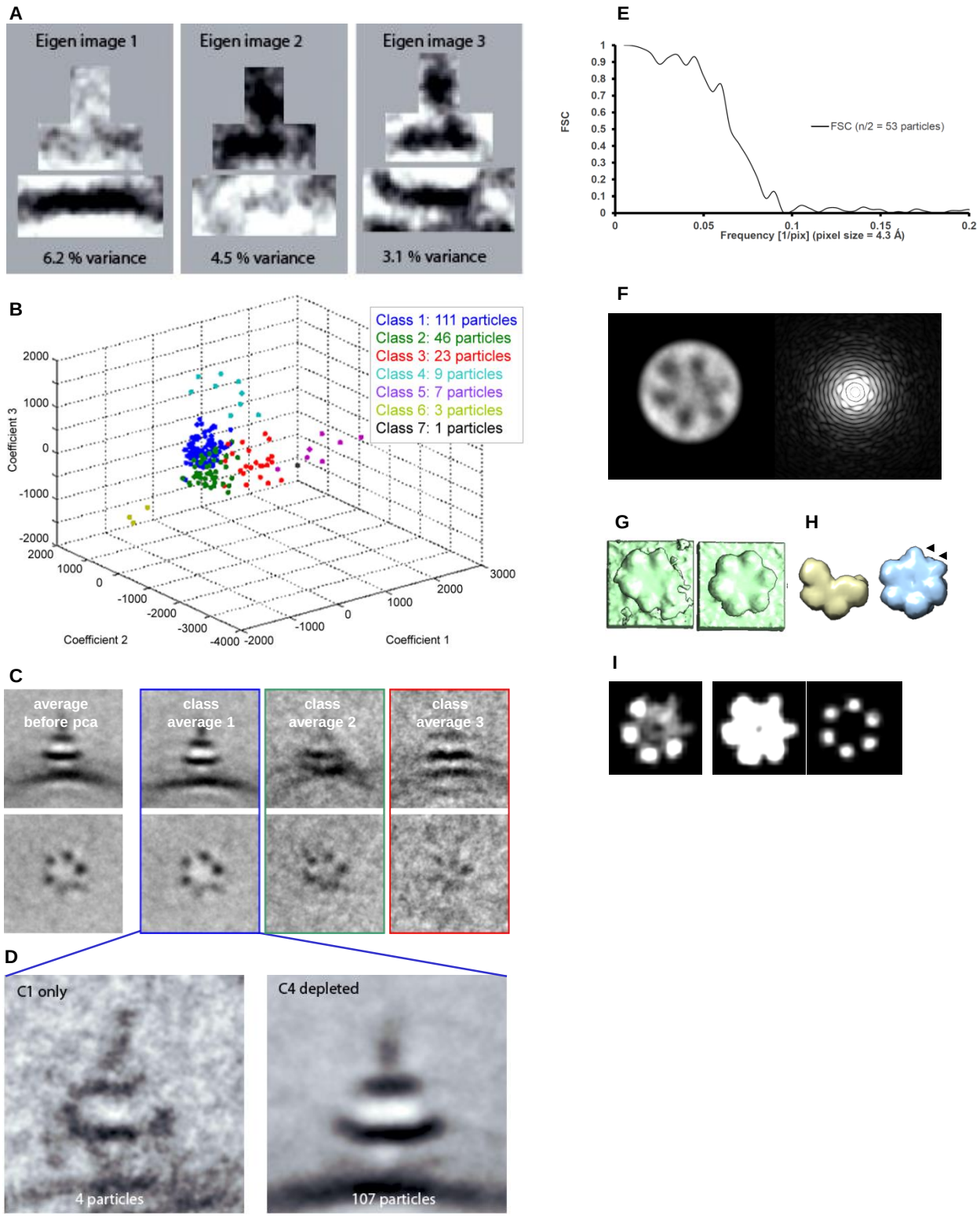
A
Eigen image 1
Eigen image 2
Eigen image 3
6.2 % variance
4.5 % variance
3.1 % variance
B
Class 1: 111 particles
Class 2: 46 particles
Class 3: 23 particles
Class 4: 9 particles
Class 5: 7 particles
Class 6: 3 particles
Class 7: 1 particles
Coefficient 3
Coefficient 2
Coefficient 1
C
average before pca
class average 1
class average 2
class average 3
D
C1 only
4 particles
C4 depleted
107 particles
E
FSC
FSC (n/2 = 53 particles)
Frequency [1/pix] (pixel size = 4.3 Å)
F
G
H
I

Fig. S4

Fig. S4

Cryo-ET analyses. (**A** to **D**) Classification of subtomograms of C1 immune complexes by principle component analysis. (**A**) First three eigenimages accounting for 14% of variation within 200 subtomograms. (**B**) K-means clustering of seven classes (defined by the optimal Bayesian optimization criterion) using first three eigenvectors. (**C**) Vertical (top row) and horizontal (bottom row) sections through the non-classified average (left panel) and first three class averages (blue, green and red). (**D**) Sections through subclasses of class 1 (111 particles) originating from DNP-liposomes incubated with anti-DNP and C1 (4 particles; left panel), or anti-DNP and C4-depleted serum (107 particles; right panel). The subclass average of these latter 107 particles was used for symmetrization, docking and resolution measurement (*20*). (**E**) Fourier Shell correlation curve of an even-odd split data set, indicating a resolution of 5 nm or 6.6 nm with 0.143 or 0.5 cut off criteria, respectively. (**F**) A 5 nm thick section through the lower platform of the unsymmetrized average cryo-ET map (left) and its Fourier transform (right) indicate the overall 6-fold symmetry allowing for symmetric averaging for modeling. (**G**) Corresponding isosurfaces of unsymmetrized (left) and symmetrized (right) cryo-ET map of the lower platform. (**H**) Examples of simulated 6 nm resolution maps of complexes with imperfect hexagonal symmetry: four IgGs with four headpieces (left) and six IgGs with four associated headpieces (right). Arrow heads indicate position of missing head pieces. (**I**) Sections through the simulated map of six IgG and four C1q headpieces at heights corresponding to the horizontal sections in Fig. 4B.

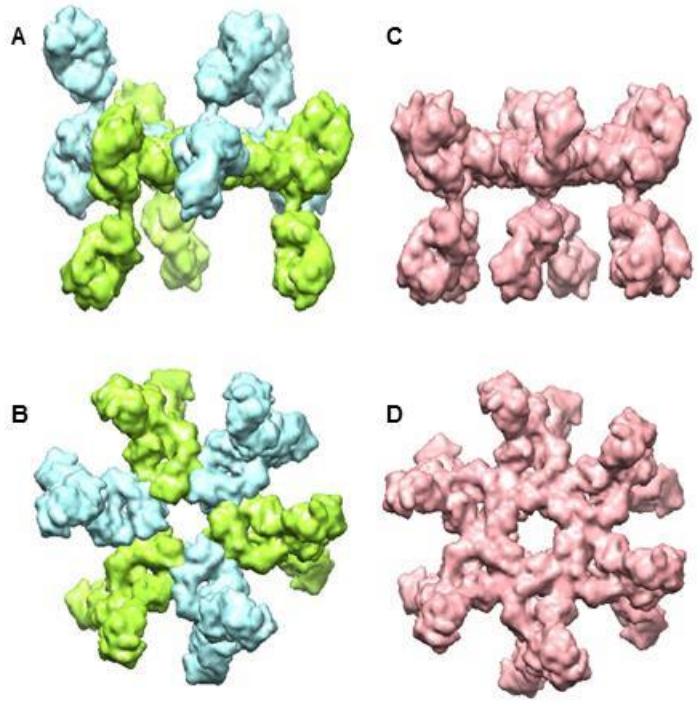

Fig. S5

Adaptation of the 1HZH IgG1-b12 hexamer structure for docking into the averaged cryo-ET density map. (**A**) Side view and (**B**) top view of 1HZH crystal packing showing alternating upwards oriented (blue) and downward oriented (green) Fab arms, with Fc segments in a central hexameric arrangement. (**C**) Side view and (**D**) top view of the adapted 1HZH structure with the upward oriented Fab segments flipped downwards (by 180° rotation around the Fc dimer axis), while keeping the hexameric arrangement in the Fc segments, resulting in six Fab arms pointing downwards and a platform comprising the other Fab arms and the Fc segments.

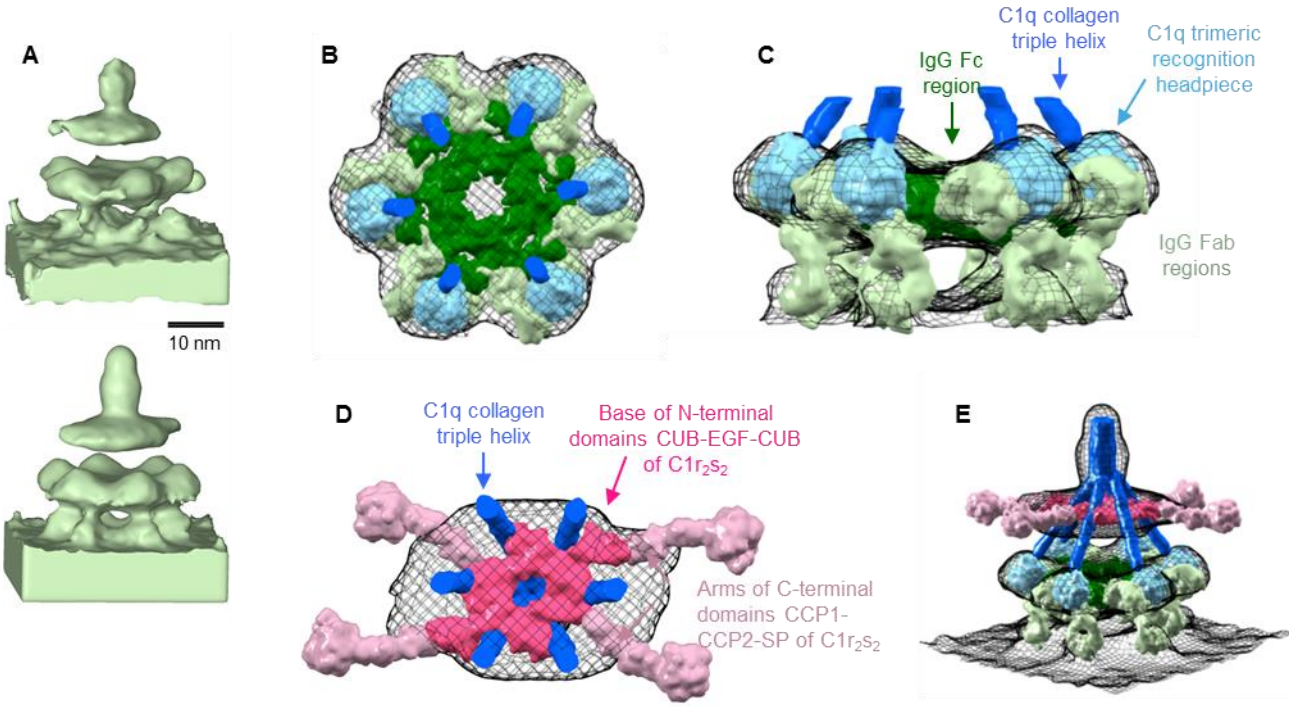

Fig. S6

Modeling the antibody-C1 complex. **(A)** Unsymmetrized (top) and symmetrized (bottom) isosurface density maps of the averaged antibody-C1 complexes. The symmetrized map was obtained by imposing six-fold symmetry to the lower platform and two-fold symmetry to the upper platform. (**B**) Top and (**C**) side view of the lower platform modeled by an IgG hexamer (green) interacting with C1q headpieces (light blue) and placed into the symmetrized ET map (black mesh). Fc segments form a hexameric ring (dark green) with Fab arms (light green) in an antigen-bound axial and an antigen-unbound equatorial orientation. Dark blue indicates the position of the collagen triple helices connected to the C1q headpieces. (**D**) $C1r_2s_2$ modeled with an N-terminal hetero-tetrameric base (dark pink) and four flexible arms exposing the serine protease domains (light pink). The electron density indicated the position of the N-terminal base, whereas the position of the proteolytic arms was unresolved. (**E**) Overview of the model with collagen stems and base (dark blue). The model was built as detailed in the Materials and Methods section (*20*).

Table S1

Apparent K_d values for C1q binding to antibody-opsonized cells. Mean K_d and SD for binding to Raji or Daudi cells opsonized with IgG1-7D8 or mutants thereof were calculated from C1q binding experiments as exemplified in Fig. 1D. Numbers of replicates and statistics are shown.

	Raji				Daudi			
Antibody	*N*[1]	Mean K_d (nM)[2]	SD[2]	Significance[3]	*N*[1]	Mean K_d (nM)[2]	SD[2]	Significance[3]
IgG1-7D8	3	6.5	3.1	n.a.	6	8.4	3.7	n.a.
I253A	3	18.6	7.9	*	4	21.5	8.0	**
I253D	3	109.1	55.0	**	4	157.4	44.2	***
I253Y	3	38.7	12.4	**	4	41.3	16.1	**
Q311A	3	9.1	3.5	n.s.	4	10.7	3.8	n.s.
H433A	3	97.9	23.3	***	4	117.5	67.0	**
N434A	3	44.9	12.5	***	4	40.4	9.7	***
H435A	3	7.3	2.3	n.s.	4	8.6	2.8	n.s.
H435R	3	4.7	1.4	n.s.	4	4.9	2.8	n.s.
K439E					2	361	81	***
S440K					2	109	87	*
K439E/S440K[4]					4	2.6	1.6	*
K439E+S440K[5]					3	3.3	0.3	n.s.
E345R					4	1.7	1.7	*

[1] Number of experiments. [2] Mean and standard deviation (SD.) were calculated from all experiments. [3] Statistics: 1 way ANOVA on log-transformed data followed by Dunnett's Multiple Comparison Posthoc Test (GraphPad Prism 5.01). Significance was calculated in comparison to the wild type IgG1-7D8: (n.a.) not applicable; (n.s.) not significant $P > 0.05$; *$P < 0.05$; **$P < 0.01$; ***$P < 0.001$. [4] Double mutant. [5] Assessed as a mixture of single mutants (1:1). The experiments were performed in a blinded fashion with coded antibody samples.

Table S2

EC_{50} (antibody concentration inducing half-maximal lysis) values for CDC of antibody-opsonized cells. Mean EC_{50} and SD for CDC of Daudi cells opsonized with IgG1-7D8 or mutants thereof were assessed in the presence of human serum. Numbers of replicates and statistics are shown.

Antibody	*N*[1]	Mean EC_{50} (µg/mL)[2]	SD[2]	Significance[3]
IgG1-7D8	5	0.48	0.11	n.a.
I253A	4	0.79	0.15	n.s.
I253D	5	3.33	1.05	***
I253Y	4	1.77	0.43	***
H310K	3	3.03	0.30	***
Q311A	4	0.42	0.12	n.s.
G385D	3	2.12	0.45	***
H433A	5	3.44	1.17	***
N434A	4	1.77	0.46	***
H435A	4	0.81	0.27	n.s.
H435R	5	0.28	0.06	**
Y436D	3	1.88	0.45	***
Q438D	3	2.61	0.38	***
K439E	4	2.34	0.38	***
S440K	4	1.78	0.46	***
K439E/S440K[4]	4	0.33	0.08	n.s.
K439E+S440K[5]	4	0.48	0.17	n.s.
K322A	4	>30[6]	n.d.	[7]
E345R	4	0.04	0.01	***

[1] Number of experiments. [2] Mean and standard deviation (SD) were calculated from all experiments. (n.d.) not determined. [3] Statistics: 1 way ANOVA on log-transformed data followed by Dunnett's Multiple Comparison Posthoc Test (GraphPad Prism 5.01). Significance was calculated in comparison to the wild type IgG1-7D8: (n.a.) not applicable; (n.s.) not significant $P > 0.05$; $^{**}P < 0.01$; $^{***}P < 0.001$. [4] Double mutant. [5] Assessed as a mixture of single mutants (1:1). [6] EC_{50} indicated as >30 µg/mL as 50% lysis was not reached. [7] This difference was considered significant although *P*-value could not be determined.

Table S3

Native mass spectrometry of the IgG1-RGY hexamer. Observed ion signals and derived molecular weights for the monomeric antibody IgG1-005, and the monomeric and hexameric species of the triple mutant IgG1-005-RGY. The experimentally measured mass of the hexamer, 890,327 Da, is within 0.1% of the expected mass of 6 times the mass of the IgG1-005-RGY monomer.

	IgG1-005		RGY	
z	m/z	Mass (Da)	m/z	Mass (Da)
29	5,107.9	147,288.1	5,123.9	148,593.1
28	5,290.0	147,336.0	5,305.2	148,545.6
27	5,485.5	147,379.5	5,501.4	148,537.8
26	5,696.3	147,427.8	5,712.2	148,517.2
25	5,924.0	147,475.0	5,940.5	148,512.5
24	6,170.7	147,520.8	6,188.1	148,514.4
Average		**147,404.5**		**148,536.8**
SD		**87.1**		**30.7**
76			11,714.8	890,248.8
75			11,870.6	890,220.0
74			12,032.6	890,338.4
73			12,196.6	890,278.8
72			12,366.5	890,316.0
71			12,540.9	890,332.9
70			12,723.2	890,554.0
Average				**890,327.0**
SD				**109.3**

Additional Author notes

Author responsibilities

PG and PWHIP conceived the project. CAD, RIK, FJB, RNdJ, KS, DRB, JS, PG and PWHIP analyzed data and wrote the manuscript. CAD and PG designed EM experiments. CAD prepared samples for EM, reconstructed and averaged tomograms. CAD and RIK collected and modeled EM data. FJB, KS, MV, JS and PWHIP designed CDC experiments. FJB and MV performed CDC analyses. DU and CAD performed negative stain EM. SR and AJRH performed mass spectrometry experiments. EOS and IAW performed IgG1-b12 structural analyses. RNdJ, EOS, IAW and DRB performed modeling and designed mutations. MAL and RPT performed C1q binding analyses. RIK, AJK, JGJvdW, IAW, DRB, JS, PG and PWHIP supervised the studies.